Determination of the dynamic and static critical exponents of the two-dimensional three-state Potts model using linearly varying temperature

Shuangli Fan and Fan Zhong*
Department of Physics, Zhongshan University, Guangzhou 510275, People's Republic of China
(Received 11 December 2006; revised manuscript received 4 September 2007; published 31 October 2007)

We employ a successive Monte Carlo renormalization group procedure in the presence of a linearly varying temperature to study the three-state ($q=3$) Potts model on square lattices. By matching correlation functions of different lattice sizes at different renormalization levels, a rate exponent r associated with the temperature sweep rate R and the correlation length exponent ν are obtained. The dynamic critical exponent z is then obtained by the scaling law $z=r-1/\nu$ derived in our method. The results of $z=2.171(62)$ for $q=3$ in this work and the previously obtained $z=2.15(13)$ for $q=2$ seem to support the extension of the "weak universality" hypothesis to dynamic critical behavior. With these calculated exponents, the dynamic scaling forms of both specific heat and order parameter at various R are presented and all the other static critical exponents are determined, which verify our method. Discussions are made on how to improve the accuracy of the estimation of the dynamic critical exponent.

DOI: 10.1103/PhysRevE.76.041141 PACS number(s): 64.60.Ht, 05.10.Cc, 75.40.Gb, 75.60.−d

I. INTRODUCTION

The theoretical framework for equilibrium critical phenomena has been well established and some predictions have been estimated in high precisions allowing high quality tests with experiments [1]. The specific heat critical exponent α and the asymptotic amplitude ratio for the scalar ϕ^4 model, for example, have been calculated up to a seven-loop expansion within renormalization group (RG) theory with proper resummations [2] and are consistent with microgravity experiments [3]. The corresponding quantities for the three-dimensional (3D) XY universality class have been determined by both six- and seven-loop expansions with a resummation algorithm [4], by Monte Carlo simulations based on finite-size scaling methods and combined with high-temperature expansions [5], and by measurements of liquid helium in a low gravity environment [6]. The three values of α obtained, for example, are respectively, 0.0112(21), 0.0146(8), and 0.0127(3), representing the state of the art. Whereas these numbers show clearly the validity of the renormalization group theory, substantial theoretical (both analytical and numerical) and experimental efforts are still needed to resolve the little discrepancy even in such a case of high precision [1].

Also established in principle has been the theoretical framework for dynamic critical phenomena and the concept of dynamic universality classes have been introduced to group different dynamic critical systems [7]. Agreement of two-loop RG results of the thermal conductivity [8] with microgravity experiments [6] has been found. Less precise theoretical results, nonetheless, could be obtained even though a systematic dynamic field-theoretical method has been developed [9]. There is a three-loop $4-d$ (d is the spatial dimensionality) expansion for the dynamic critical exponent z of a N-component vector order parameter with $O(N)$ symmetry [10]. Up to now the longest theoretical expansion is a four-loop $4-d$ expansion for z of model A with only a scalar order parameter [11]. It gives, for the 3D Ising model, $z=2.0237(55)$ which agrees with results of Monte Carlo simulations [12] and our varying-field renormalization-group theory [13], and, for the 2D kinetic Ising model, $z=2.0842(39)$, which is a little smaller than the current value of about 2.17 [13–15]. Thus further analytical and numerical work is still needed even for this simplest model.

A simple extension of the Ising model is the q-state Potts model [16]. The continuous field version of the model, however, contains a trilinear term and thus should show discontinuous transitions qualitatively distinct from the Ising model [17]. Nevertheless, it has been proved rigorously that the 2D Potts model, when $q\leq 4$, exhibits continuous phase transitions in the presence of temperature driving [18]. The Potts model can describe a lot of transitions and thus has many applications. Examples include the isotropic to nematic transition of liquid crystals [19], the martensitic transition in β tungsten [20], percolation problems [21], the Yang-Lee edge singularity [22], the Edwards-Anderson model of spin glasses [23], and quantum field theory models in particle physics [24]. The 2D $q=3$ model to be studied here, in particular, can be used to describe phase transitions of krypton absorbed on graphite [25]. As one of the most studied models, there have been yet few exact results for this model [26,27]. Three-loop $6-d$ expansions with proper resummations for the static critical exponents of the Potts model have been compiled [28], allowing for possible comparisons with experiments. These results, however, are not expected to be close to the corresponding exact values at two dimensions. Moreover, there has not yet been dynamic field theory for the dynamic properties of the model, though for the 2D three-state Potts model, various other approaches exist to calculate its dynamic critical exponent [29–47] and we will make a brief account in the following.

A first calculation of the dynamic critical exponent of the 2D three-state Potts model used a Migdal-type recursion method generalized to dynamics [29], yielding $z=1.92$ or 2.25 when the series expansion results and the corresponding

*Corresponding author. stszf@mail.sysu.edu.cn

scaling relation were utilized, respectively. Measuring the nonlinear relaxation exponent Δ^{nl} of the magnetization gave rise to $z=2.41$ with the aid of the scaling relation $z=(\Delta^{nl}+\beta)/\nu$ [30]. The first dynamic Monte Carlo renormalization group (MCRG) method applied to the model at its critical temperature led to $z=2.7\pm0.4$ [31], which was also found by a modified MCRG [32]. However, when data of earlier times were included, z becomes close to the value 2.1–2.3 that was found by the same authors later using a finite size scaling method [33]. On the basis of hyperscaling, a scaling relation $z\nu=2+\alpha$ for the two-dimensional Ising and Potts model was predicted [34]. It produces a value of 2.8 for z that is close to the early MCRG result. However, by comparing the magnetization of the original and the renormalized one in the modified dynamic MCRG scheme [48] with lattice sizes as large as 800×800, z was calculated to be 2.43 ± 0.15 [35]. Subsequent work improved the precision. By fitting the equilibrium relaxation functions for energy and order parameter to a sum of exponential decays and using the finite-size dependence at T_c, z was obtained as $z=2.17\pm0.04$ [36]. Power-law relaxation of the magnetization in lattice sizes up to 1200×1200 directly resulted in $z=2.16\pm0.04$ using the exact results for the static critical exponents [37]. Yet another dynamic finite-size scaling analysis of the relaxation times gave $z=2.18\pm0.04$ with the relaxation times being obtained by the collapse of the time-dependent magnetization squared of different system sizes [38]. Another method to determine the dynamic exponent was by making use of the short-time scaling behavior of the critical dynamics [49]. From the power law behavior of the physical observables at the beginning of the time evolution, the dynamic critical exponent could be determined. A heat bath algorithm was employed in Ref. [39] and with the short-time analysis of the autocorrelation function the result was $z=2.1983(81)$. By taking into account the microscopic time scale that the system needed to enter a macroscopic quasistable state [40], the results were $z=2.196(8)$ (heat-bath algorithm) and $z=2.198(13)$ (Metropolis algorithm). The greater efficiency of the heat-bath algorithm in the short time dynamics was also revealed. The same simulations with the heat-bath algorithm were carried out on triangle lattices [41] and the dynamic critical exponent was 2.191(6), which was consistent with those on square lattices [39,40] and verified the universality of the short-time dynamics. By searching for the best fit of collapse of the fourth-order Binder cumulant and the second moment of the magnetization, the results were $z=2.203(11)$ and $z=2.191(1)$, respectively [42,43]. By submitting the system to different initial conditions and combining the behavior of the order parameter and its second moment, z was obtained to be 2.197(3) [44], which was compatible with those found in [39–43] very well. We note that there were specifically designed cluster algorithms such as Swendsen-Wang and Wolff algorithms [45–47] that could produce unusually small z resulting from the greatly reduced relaxation times.

At the present situation concerned, several issues emerge. First, one has to conclude that the dynamic critical exponent of the 2D three-state Potts model is still scattered. There are mainly three catalogs of values. One is around 2.4 obtained mainly from dynamic MCRG and some other methods [29–33,35]. Another is about 2.17 from the scaling of equilibrium relaxation times and the like [36–38]. The other is 2.20 or so from short-time critical behavior [39–44]. Though there is a slight overlap within statistical errors for the latter two catalogs, the results from the dynamic MCRG appear a little far apart even for quite large lattices [35]. This necessitates a reinvestigation of the MCRG kind methods. Moreover, except for the last catalog, the other two suffer from the notoriously critical slowing down. Indeed, since the system is simulated at the critical temperature, critical slowing down is a major concern for accurately detecting the equilibrium properties of the system. A further issue concerns the idea of "weak universality" [50] extended to the dynamic critical behavior for the 2D Potts model, namely, z is the same for $q=2$, $q=3$, and $q=4$ [36]. Although there are agreements on this [35–37], the debate on the q independence still exists [44]. Thus in this paper, the successive MCRG procedure we have successfully used in the 2D Ising model [51] is applied to the 2D three-state Potts model with greater numerical efforts to calculate both dynamic and static critical exponents. This nonequilibrium method can effectively overcome the critical slowing down which appears in equilibrium situations. In this way, we can compare the dynamic critical exponent with that in Ref. [51] for the 2D Ising model that is equivalent to the $q=2$ Potts model and investigate the reliability of the dynamic universality class, since $q=3$ was suggested to be slightly different from $q=2$ and 4 in the weak universality scheme [36]. Furthermore, the dynamic scaling form of the specific heat obtained from the fluctuation-dissipation theorem in the nonequilibrium conditions is presented as an additional outcome of the method. Dependence of the variances of the energy and the order parameter on the lattice size and the sweep rate are also respectively discussed in order to improve the accuracy of our method.

The renormalization group theory was first introduced to the study of critical phenomena by Wilson [52]. It was then incorporated with Monte Carlo simulations by Ma [53] and developed by Swendsen [54] to study both static and dynamic critical phenomena. A dynamic successive MCRG was proposed by Tobochnik and co-workers [55] and extended by Katz and co-workers [56], where the dynamic exponent z was obtained by matching correlation functions at different blocking levels at different times. It was further extended to include two variables in the case of the 2D Ising model below its critical temperature T_c and in the presence of a linearly varying magnetic field, and it was found that the dynamic scaling behavior of hysteresis was originated from a rate exponent r that characterized the response of the system to the sweep rate of the field driving the transition [57]. The exponent r related the original sweep rate R of the external field to the renormalized one by $R^{(1)}=Rb^r$, where b was the scaling factor. Also the scaling of thermal hysteresis with temperature scanning rate for first-order phase transitions was studied [58]. A linearly varying temperature was applied to the 2D Ising model near its criticality [51]. By implementing the successive MCRG procedure, both dynamic and static exponents were obtained, which were in agreement with existing results. Recently, a field theoretical version of the RG theory was developed to treat analytically the linearly varying field and temperature [13], which proved the validity

of the method. Owing to the nonequilibrium driving, the method can effectively overcome the critical slowing down and can thus be an alternative method for determining critical exponents efficiently.

The rest of the paper is organized as follows: In Sec. II, we introduce the 2D Potts model and the dynamic MCRG technique. Section III contains the results and data analysis, which proceeds like this. First, the critical temperature is obtained by fitting the simulated transition temperature for different sweep rates. The correlation functions are then matched at different blocking levels at different times to obtain the correlation length exponent ν and the additionally introduced exponent r. Then the dynamic critical exponent z is obtained via $z=r-1/\nu$. As our main aim is to determine z and confirm its q independence, we will verify the accuracy of the estimations of the exponents and determine all the other static critical exponents simultaneously. According to the scaling relation $\alpha=2-d\nu$, the specific heat exponent α is obtained. By virtue of the calculated exponents, the specific heat and the temperature are rescaled and the corresponding collapsed curves for different system sizes and sweep rates are presented, which verifies the dynamic scaling form of the specific heat and the reliability of the exponents obtained. Moreover, a good estimation of the order parameter exponent β is made by the collapse of the rescaled order parameter vs the rescaled temperature with the previously obtained exponents. Having two independent static exponents ν and β in hand, we can determine other static exponents according to the known scaling laws. The influence of the sweep rate on both specific heat and order parameter is discussed. To improve the accuracy of the method on the whole, we discuss the variations of the energy and the order parameter variances with different lattice size and sweep rate. A summary of our results is made in Sec. IV.

II. MODEL AND METHOD

We consider the three-state Potts model on a two-dimensional square lattice. The Hamiltonian of the Potts model is defined as

$$H=-\sum_{\langle i,j\rangle}\delta_{\sigma_i\sigma_j}, \tag{1}$$

where δ is the Kronecker delta function, and $\langle i,j\rangle$ denotes the sum over nearest-neighbor spins. We use J as an energy scale and set $J=1$ for simplicity. The spin variable σ_i of this model can take on three different values, i.e., $q=3$. The order parameter is defined as

$$\langle M\rangle=(qN_{\max}/N-1)/(q-1), \tag{2}$$

where $N_{\max}=\max(N_1,N_2,\ldots,N_q)$. N_q is the number of spins in state q and N is the total number of spins. The specific heat per site is

$$C=\frac{L^d}{T^2}(\langle E^2\rangle-\langle E\rangle^2), \tag{3}$$

where L and d indicate, respectively, the size and the dimensionality of the system. $\langle E^2\rangle-\langle E\rangle^2$ is the fluctuation of the internal energy per site. The nearest-neighbor spin-spin correlation function is

$$G_{nn}=\left\langle\frac{1}{2N}\sum_{\langle i,j\rangle}\delta_{\sigma_i\sigma_j}\right\rangle-\langle M\rangle^2. \tag{4}$$

We use dynamic MCRG to study the Potts model in the presence of a linearly varying temperature field $T=Rt$, where t is the time that is measured by Monte Carlo steps per spin. In each step all the spins are tested sequentially to flip or not according to the Metropolis algorithm [59]. We start with a ground state that is set to be one of the three equivalent states. As heated from zero temperature to that above the critical temperature, the system undergoes a transition from the ordered state to a disordered one. In each Monte Carlo step, the successive MCRG procedure is carried and M, E, and G at various renormalization levels are recorded and subsequently averaged over many different independent runs. Matching correlation functions at different renormalization levels with the same size can then give rise to both dynamic and static critical exponents. The whole procedure has been discussed explicitly in Ref. [51] and we will only make a brief account here.

During the MCRG procedure, b^d spins are replaced by a new block spin which is determined by the majority rule. The renormalized T, R, and t are denoted by $T^{(m)}$, $R^{(m)}$, and $t^{(m)}$, respectively. Here m indicates the mth iteration of the renormalization procedure. After renormalization, the three parameters flow to their corresponding new ones, which can be expressed as

$$(T-T_c)^{(1)}=(T-T_c)b^{1/\nu}, \tag{5}$$

$$R^{(1)}=Rb^r, \tag{6}$$

$$(t-t_c)^{(1)}=(t-t_c)b^{-z}, \tag{7}$$

where t_c is the time at which $T=T_c$. Combining the three equations above with $T=Rt$ we obtain the scaling law [13,51,57]

$$1/\nu=r-z, \tag{8}$$

from which the dynamic critical exponent can be obtained once r and ν are known.

To this end, correlation functions of two block spin systems with the same size are matched in order to reduce the size effect, that is,

$$G_{nn}[L,m,R_s^{(m)},T_{ps}^{(m)}-T_c]=G_{nn}[Lb,m+1,R^{(m+1)},T_p^{(m+1)}-T_c], \tag{9}$$

where T_p is the dynamic transition temperature that corresponds to the peak value of the correlation function G_{nn} and the subscript s indicates the small lattice. From Eqs. (5), (6), and (9) one sees that

$$R_s^{(m)}=R^{(m+1)}=R^{(m)}b^r, \tag{10}$$

and

$$T_{ps}^{(m)}-T_c=T_p^{(m+1)}-T_c=(T_p^{(m)}-T_c)b^{1/\nu}. \tag{11}$$

Therefore

$$r = \ln(R_s^{(m)}/R^{(m)})/\ln b, \tag{12}$$

and

$$\nu = \ln b/\ln[(T_{PS}^{(m)} - T_c)/(T_p^{(m)} - T_c)]. \tag{13}$$

Other critical exponents can also be obtained. With the present exponent ν, the related exponent α can be determined by the scaling law $\alpha = 2 - d\nu$. According to the renormalization group theory [60], the specific heat and the order parameter in the vicinity of the critical region can be cast into the following scaling forms:

$$C(T - T_c, R) = R^{-\alpha/r\nu} f_1((T - T_c)R^{-1/r\nu}), \tag{14}$$

$$M(T - T_c, R) = R^{\beta/r\nu} f_2((T - T_c)R^{-1/r\nu}), \tag{15}$$

where f_1 and f_2 are universal scaling functions. Equation (15) thus implies that β may be determined by seeking a good collapse of the rescaled order parameter.

One still needs the critical temperature T_c in the procedure described above. As the system is driven by a linearly varying temperature $T = Rt$, its response to the temperature is controlled by the sweep rate R. So it is clear that there is a hysteresis in the transition temperature. It is just the hysteresis of this kind that overcomes the critical slowing down. Each R has its own T_p and increasing R leads to a larger deviation of T_p from T_c. Note that as R approaches zero, the transition from the ordered to the disordered state ought to approach the equilibrium transition that takes place at T_c. Moreover, at equilibrium, the peak of the correlation function is just at T_c. Accordingly, we expect

$$T_p = T_c' + aR^n \tag{16}$$

with T_c' necessarily equal to T_c, where a and n are fitted parameters. This then provides a method for determining T_c.

III. RESULTS AND DISCUSSIONS

We select the large and small lattice pairs to be 512×512 and 256×256, respectively, and the scaling factor $b = 2$. The nearest-neighbor correlation function, the specific heat, and the order parameter are calculated and all these quantities are averaged over 200–4000 independent runs.

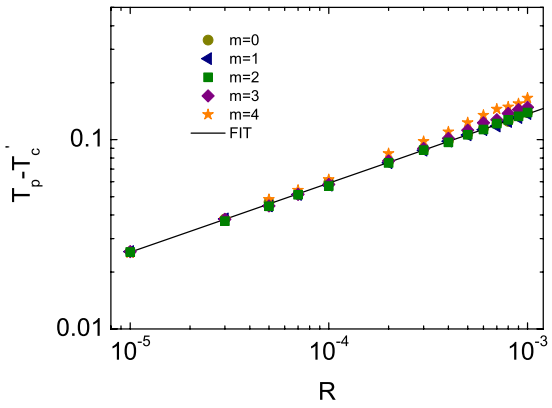

FIG. 1. (Color online) Log-log plot of $T_p - T_c'$ vs R of the small lattice. The straight line is the power law fit of data when $m=0$ and $m=1$.

A. The critical temperature T_c

Fitting of T_p vs R of the small lattice ($m=0$ and $m=1$) yields $T_c' = 0.9968(20)$, $a = 1.704(106)$, and $n = 0.365(11)$. As expected, T_c' is consistent with the exact result $T_c = 1/\ln(1 + \sqrt{3}) \approx 0.995$ very well. Since there is little difference between the fitted critical temperature and the exact one, we will use the latter hereafter.

Figure 1 shows the log-log plot of $T_p - T_c'$ vs R of the small lattice. The straight line is the power law fit of data when $m=0$ and $m=1$. For R not greater than 10^{-4}, the data points of different iterations coincide with each other very well. With the increasing of R, the more iterations lead to more obvious deviations. So R should be sufficiently small in order not to be too far away from the fixed point. In other words, the accuracies of the fitted transition temperature and parameters in Fig. 1 are to some extent restricted by the range of R, while the range of R is restricted by the computer running time.

B. The exponents obtained by the dynamic MCRG procedure

Table I shows our calculated exponents according to the dynamic MCRG procedure. R in the first column indicates the sweep rate of the temperature of the large lattice, which varies from 0.000 01 to 0.0005. Five iterations were carried

TABLE I. The exponents obtained by successive renormalization group approach.

	$m=1$				$m=2$				$m=3$				$m=4$			
R	ν	r	z	$1/r\nu$	ν	r	z	$1/r\nu$	ν	r	z	$1/r\nu$	ν	r	z	$1/r\nu$
1×10^{-5}	0.695	3.978	2.539	0.362	0.826	3.264	2.053	0.371	0.866	3.407	2.251	0.339	0.851	3.370	2.195	0.349
3×10^{-5}	0.705	3.889	2.469	0.365	0.784	3.362	2.086	0.380	0.793	3.430	2.169	0.368	0.838	3.378	2.185	0.353
5×10^{-5}	0.696	3.856	2.419	0.373	0.770	3.517	2.219	0.369	0.796	3.400	2.143	0.370	0.836	3.291	2.095	0.363
7×10^{-5}	0.707	3.819	2.405	0.370	0.806	3.506	2.266	0.354	0.818	3.380	2.157	0.362	0.818	3.389	2.166	0.361
1×10^{-4}	0.723	3.816	2.432	0.363	0.784	3.498	2.222	0.365	0.821	3.442	2.224	0.354	0.836	3.328	2.131	0.360
3×10^{-4}	0.718	3.764	2.372	0.370	0.771	3.513	2.216	0.369	0.764	3.459	2.150	0.378	0.798	3.434	2.182	0.365
5×10^{-4}	0.714	3.751	2.349	0.374	0.752	3.530	2.2001	0.377	0.760	3.474	2.158	0.379	0.755	3.388	2.063	0.391

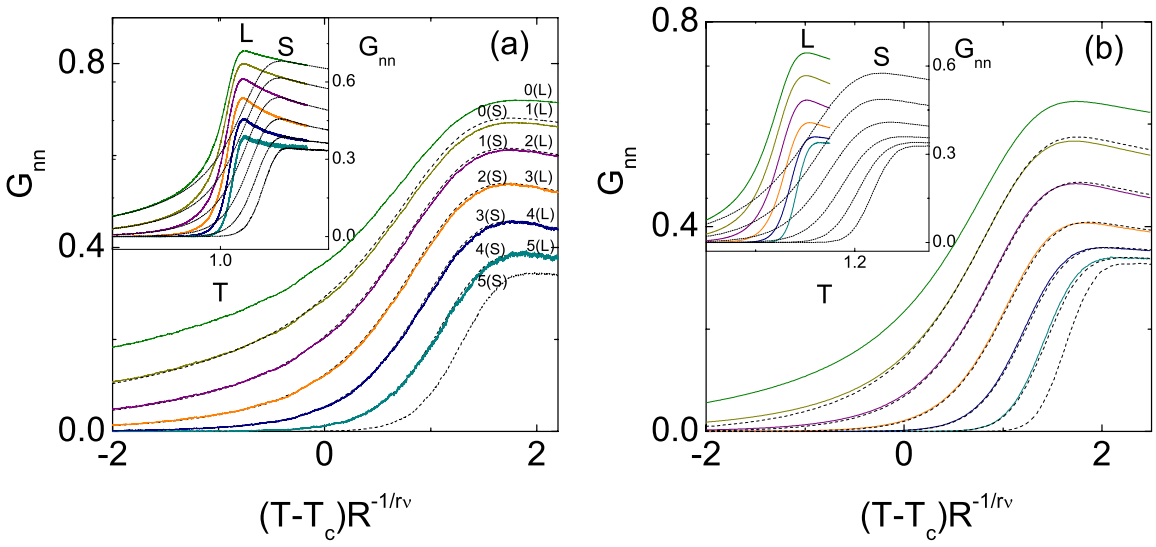

FIG. 2. (Color online) The correlation function G_{nn} vs the rescaled temperature $(T-T_c)R^{-1/r\nu}$ for the small lattice (dashed lines) and the large lattice (solid lines). "L" and "S" above the curves indicate the large and small lattices, respectively. Insets show G_{nn} vs T, where the peak locations of G_{nn} are almost constant for each lattice size. The sweep rates of the large lattice are 0.000 01 in (a) and 0.0005 in (b). The numbers above curves of (a) denote the number of iterations of the RG procedure. Situations in (b) and the two insets are the same as in (a) and have not been labeled.

out on the two lattices and the parameter m in the table indicates the mth iteration of the renormalization procedure of the large lattice. From the table we see that r is positive, which means that the renormalized sweep rate will be greater than the original one. In other words, R is a relevant variable. The flow of parameters as renormalizations in the parameter space may be inferred by the exponents in Table I. When $m=1$, irrelevant variables are still prevalent and the corresponding exponents show large deviations from their respective fixed point values given below. After the irrelevant variables have been iterated away, the system approaches the fixed point. As a result, the exponents almost remain constant within statistical errors and thus reflect the properties of the fixed point involved. Further iterations will drive the system away from the fixed point since R is a relevant variable, which conforms with Fig. 1. Consequently, we only present the exponents calculated from $m=1$, 2, 3, and 4 in Table I and calculate average values over the second, third, and fourth renormalization, yielding $\nu=0.802(33)$, $r=3.417(74)$, $z=2.168(59)$, and $1/r\nu=0.365(23)$. The dynamic exponent obtained in this way is consistent with those in Refs. [36–38].

The deviation of $\nu=0.802$ from the exact one ($\nu=5/6 \approx 0.833$) is within the statistical error. Comparing $1/r\nu$ obtained from the successive MCRG approach with the hysteresis exponent n from Eq. (16), one finds they are compatible with each other very well and in agreement with previous results [13] and prove the validity of the scaling law $z=r(1-n)$ [51].

We only matched the peak values of the correlation functions of the large and small lattices to find the exponents in Table I. To be consistent, however, all the correlation functions of the two lattices ought to be matched. According to the renormalization group theory, the sweep rate R flows to $R^{(1)}=Rb^r$ when the system is renormalized. For a certain sweep rate R for the large lattice, its renormalized correlation function will match that of the small unrenormalized lattice whose sweep rate is Rb^r. Since $(T-T_c)^{(1)}=(T-T_c)b^{1/\nu}$, we let $b=R^{-1/r}$ so that the rescaled temperature is $(T-T_c)R^{-1/r\nu}$. Figure 2 shows the matching of the two lattices with $R_1=0.000\,01$ and $R_2=0.0005$, respectively. The corresponding sweep rates of the small lattice are $R_1b^r=0.0001$ and $R_2b^r=0.0053$. Five iterations of the RG procedure were carried on both lattices. The solid and dashed lines from top to bottom correspond to $m=0-5$, respectively. From Fig. 2 we can see that the peak values of the correlation functions decrease when increasing both the renormalization level and the sweep rate. Increasing the sweep rate, especially that of 0.0053 of the small lattice in Fig. 2(b) thus leads to less distinguishable peak values, which in turn lead to less reliable exponents calculated according to the successive MCRG. For sufficiently small sweep rates such as those in Fig. 2(a) the matching of the two lattices is desirable except when $m=1$, consistent with the averages above. Although the matching in Fig. 2(b) is not as good as that in Fig. 2(a), it is, nevertheless, acceptable. Consequently, the upper limit of the sweep rate in Table I is acceptable, too. Note that $m=0$ of the large lattice and $m=5$ of the small lattice are not expected to coincide with others.

The above paragraph shows the reliability of the correlation function matching, which is essential for our calculations. Since no analytic result for the dynamic critical exponent z has yet been calculated for the model concerned and the existing numerical ones are scattered, it is necessary to verify the reliability and accuracy of the estimation of z, which is also important for solving the debate on its q independence. In our work, the dynamic critical exponent z is obtained via the scaling relation $z=r-1/\nu$ that has been confirmed analytically, the accuracy of the estimation of z de-

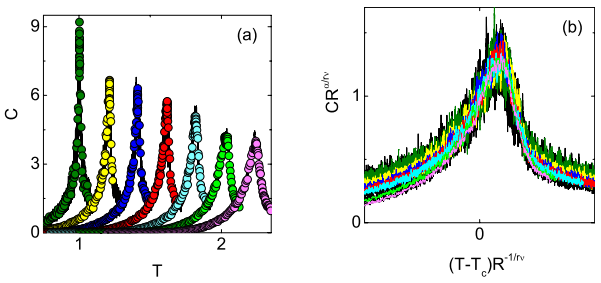

FIG. 3. (Color online) (a) Temperature dependence of the specific heat for the large lattice (solid lines) and the small lattice (filled circles). Sweep rates from the left to right are 0.000 01, 0.000 03, 0.000 05, 0.000 07, 0.0001, 0.0003, and 0.0005, respectively. Curves except that of $R=0.000\ 01$ have been shifted along the horizontal coordinates by 0.2, 0.4, 0.6, 0.8, 1.0, and 1.2 for clarity. (b) The rescaled specific heat $CR^{\alpha/r\nu}$ vs the rescaled temperature $(T-T_c)R^{-1/r\nu}$ for different R. The range of R and the plot types are the same as those in (a) except that the lines for the small lattice are dashed.

pends on those of r and ν. Then in the following two subsections we will discuss the reliability of the estimations of r and ν and determine all the other static critical exponents simultaneously.

C. The specific heat exponent α

Applying the exponent ν calculated in Table I to the scaling law $\alpha=2-d\nu$, one obtains the specific heat exponent $\alpha=0.396(66)$, which is consistent with the exact one $\alpha=1/3$ within statistical error. We may check the reliability of the calculated α and $1/r\nu$ by Eq. (14). Figure 3(a) shows the temperature variations of the specific heat with various sweep rates, where some data of the small lattice have been removed for clarity. Figure 3(b) exhibits the data collapsing of the specific heat in the vicinity of the critical region for different R, which confirms our results.

Several remarks are in order here. First, the system exhibits larger fluctuations for smaller sweep rates, as it becomes more equilibriumlike. But for R around 0.000 01, we have averaged only over 200 samples. This is the reason for the large curve width in Fig. 3(b), and thus the collapse in it is not so bad. Second, the specific heat was obtained from the fluctuation-dissipation theorem in Eq. (3). This equation applies to the static case [61], where $\langle E\rangle$ and $\langle E^2\rangle$ are averages of equilibrium states, while in our dynamic case they are both ensemble averages. Thus possible systematic deviations, especially when the sweep rate getting larger, may appear due to the violation of the theorem. Another factor is the possible finite-size effect. Usually this effect renders the divergences at criticality rounded and shifted. An indication of it can be seen in Fig. 3(a), namely, for small rates, the specific heat curves of the two lattices with the same R do not exactly coincide with each other near the transition point, i.e., around the peak values of the specific heat (not because of the removal of some data as mentioned above). In the present case, however, the rounding, shifting, and the coincidence of the specific heat in Fig. 3(a) may result from the linearly varying temperature that imposes an external time scale for the system to follow. Consequently, the peak values of the specific heat in Fig. 3 decrease and the corresponding transition temperatures increase with increasing R. It should also be pointed out that the possible finite-size effect appearing here ought to have a negligible effect on the results in Table I, where the matching is between two lattices with the same size.

D. The order parameter exponent β

Figure 4 shows the temperature dependence of the order parameter of the two lattices with various R. With the decreasing of R, the behavior of the order parameter near the critical region is more analogous to the equilibrium case that shows finite-size effect. For an infinitesimal R the curve will be identical to that of the equilibrium phase transition, while increasing R will lead to better and better data collapsing of the two lattices sharing the same R, i.e., less finite-size effect. This is compatible with that in Fig. 3(a). The collapsed curves of the rescaled order parameter according to Eq. (15) by using the exact and conjectured values of β are shown in Fig. 4(b). Less diffusivity of the collapsed curve means more

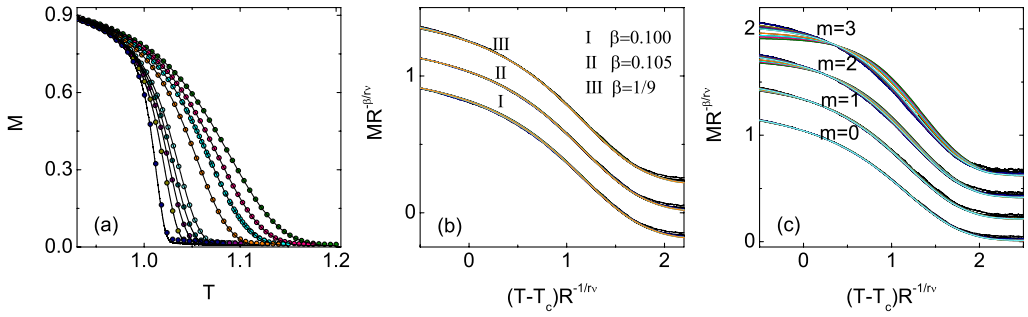

FIG. 4. (Color online) (a) Temperature dependence of the order parameter of the large lattice (solid lines) and the small lattice (filled circles). Curves from left to right correspond to R of 0.000 01, 0.000 03, 0.000 05, 0.000 07, 0.0001, 0.0003, 0.0005, 0.0007, and 0.001, respectively. (b) The rescaled order parameter $MR^{-\beta/r\nu}$ vs the rescaled temperature $(T-T_c)R^{-1/r\nu}$ for $m=0$. The upper and bottom curves are respectively shifted along the vertical coordinates by +0.2 and −0.2 for clarity. (c) The rescaled order parameter $MR^{-\beta/r\nu}$ vs the rescaled temperature $(T-T_c)R^{-1/r\nu}$ for $\beta=0.108$ and $m=0$, 1, 2, and 3, respectively. The curves corresponding to $m=1$, 2, and 3 are shifted along the vertical coordinates by 0.2, 0.4, and 0.6, respectively. The lattice size and the range of R in (b) and (c) are the same as those in (a).

accuracy of β. As a rough estimate, we average over $\beta=1/9\approx0.111$ and $\beta=0.105$ to get $\beta=0.108(4)$ [51]. Figure 4(c) ($\beta=0.108$) shows that when $m=0$ and $m=1$, the collapsing of the curves are very good. With the increasing of m, the situation becomes worse. For example, when $m=3$ the collapsed curve is separated into two parts. The upper part near the critical region corresponds to the sweep rate that ranges from 0.000 01 to 0.0001. The bottom part corresponds to 0.0003 to 0.001. This is because the renormalized sweep rate $R^{(m)}$ becomes larger and larger as m increases, giving rise to more deviation of the order parameter from the dynamic scaling form due to the deviation from the fixed point. When the sweep rate is sufficiently small (ranging from 0.000 01 to 0.0001), the coincidence of the rescaled parameter is desirable for each curve.

This then gives us a better estimate of the relevant exponents. Indeed, from Table I we may well average the exponents over the sweep rates from 0.000 01 to 0.0001, leading to $\nu=0.816(27)$, $r=3.398(74)$, $1/(r\nu)=0.361(10)$, $z=2.171(62)$, and $\alpha=0.368(54)$. Moreover, the scaling plots will become better for this restricted range of sweep rates. And because of the small rates used, corrections to scaling [62] ought to be small too. In fact, we have used a wider range only to show the validity of the theory. With the obtained static exponents $\nu=0.816(27)$ and $\beta=0.108(4)$, other static exponents can be determined by the scaling laws. The results are $\gamma=1.416(62)$, $\delta=14.1(1.1)$, and $\eta=0.265(19)$, respectively. The corresponding exact ones are $\gamma=13/9\approx1.444$, $\delta=14$, and $\eta=4/15\approx0.267$. Our results thus agree well with the exact ones within statistical errors and confirm the validity of our method in determining both dynamic and static critical exponents.

E. Variance analysis

The main results of this work have been discussed in the preceding subsections and the validity of our method is thus verified. Aside from the validity of a method, improving the accuracy is another important issue in simulations. The exponents in Table I are obtained by matching the correlation functions, where the correlation function, according to the definitions in Sec. II, is calculated by $G_{nn}=-\langle E\rangle/2-\langle M\rangle^2$. The energy per site and the order parameter are measured by averaging over many independent samples. To improve the accuracy of the exponents, it is necessary to improve the accuracies of E, M, and then G_{nn}. So we should discuss the variance of E and M, i.e., the sample to sample fluctuations. In an equilibrium situation we observe a quantity A in n independent observations and calculate the error

$$\Delta_A(n,L)=\sqrt{(\langle A^2\rangle-\langle A\rangle^2)/n}, \tag{17}$$

with $n\gg1$. Depending on whether $\Delta_A(n,L)$ tends to zero or not in the thermodynamic limit, the system exhibits either self-averaging or lack of self-averaging, respectively [63]. In the former case we can improve the accuracy of the observable by increasing the system size, while in the latter case the only way is using more samples. In this work we are dealing with the nonequilibrium situation and both $\langle A^2\rangle$ and $\langle A\rangle$ are ensemble averages. Here we concentrate on the temperature

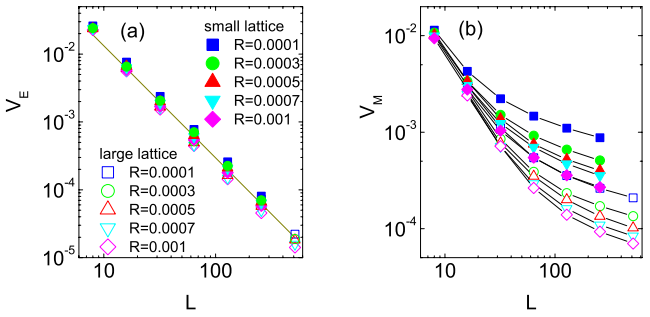

FIG. 5. (Color online) Double logarithm of the peak values of (a) V_E and (b) V_M vs L. The filled symbols are for the small lattice and the open symbols are for the large lattice. The straight line in (a) is the fit of the two lattices from $m=0$ to $m=5$ for the sweep rates shown. The sweep rates in the legends in (a) correspond to the unrenormalized ones and they apply to (b) too. Solid lines in (b) are just guides to the eye.

variation of $V_A=\langle A^2\rangle-\langle A\rangle^2$, which reaches a peak value at the transition point. In our simulations there are two controllable parameters, the lattice size L and the sweep rate R. Each iteration of the renormalization group procedure leads the system size to be b times smaller than the preceding one and we can analyze the size dependence and the sweep rate dependence of the variance concerned.

Figure 5(a) shows the peak values of V_E of different iterations vs the system size. For a certain unrenormalized lattice size with a certain unrenormalized sweep rate, the variance of the energy for $m=0-5$ are denoted by the same symbol. The straight line is the fit of all the data points presented for the two lattices with $V_E\sim L^{-\rho_E}$ and $\rho_E=1.66(31)$, consistent with $\rho_E=2(1-\alpha)/\nu=1.6$ in the equilibrium situation. Therefore V_E tends to zero in the thermodynamic limit and for a fixed number of samples the accuracy can be well improved by increasing the lattice size. Since the fit is from $m=0-5$ for various unrenormalized sweep rates, there must be some discrepancy resulting from the larger and larger renormalized sweep rates. Another factor is the restricted lattice sizes used. Nevertheless, the fit is good for the lattice sizes and the sweep rates concerned here and we can get a rough idea about the self-averaging of the nonequilibrium situation.

Figure 5(b) is the double logarithm plot of the peak values of V_M vs L. Note that the susceptibility χ could be obtained if the variance of the order parameter was multiplied by L^d/T. And just like the specific heat and the order parameter, the rescaled susceptibility $\chi R^{\gamma/r\nu}$ vs the rescaled temperature $(T-T_c)R^{-1/r\nu}$ of different sweep rates could collapse onto a single curve around the critical region. The not-perfectly straight lines in Fig. 5(b) indicate the violations of a simple power law of $V_M\sim L^{-\rho_M}$ in equilibrium situations and we only give a qualitative description here. From Fig. 5(b), it can be seen that for the large and small lattices with an equal unrenormalized sweep rate, V_M decreases with increasing lattice sizes, which means that the order parameter also exhibits self-averaging, while for a certain lattice size, V_M increases dramatically with decreasing sweep rates. This accounts for the violation of V_M from the simple power law with respect to the lattice size. More iterations lead to smaller renormal-

ized lattice sizes (so an increasing V_M) but larger renormalized sweep rates (so a decreasing V_M) and the influence of R on V_M becomes more and more negligible and V_M of different sweep rates get approximately to a constant at $L=8$. We also note that there is coincidence of V_M between the two lattices with the same sizes from $L=256$ to $L=16$, with unrenormalized sweep rate of the small lattice being $R_S=0.001$ and that of the large lattice $R_L=0.0001$. Tracing the hysteresis exponent r estimated in Sec. III A we can obtain that $R_L^{(1)} \approx R_S$, which just explains the coincidence here.

Summarizing, for a certain sweep rate we can improve the accuracies of E and M significantly by increasing the lattice size. Then the accuracy of the correlation function G_{nn} is improved. In terms of the renormalization group procedure, the more iterations lead to smaller lattice sizes and larger sweep rates and then larger fluctuations of the energy and the order parameter. These fluctuations will affect the correlation function and then the estimations of the exponents in Table I. So the iteration number m cannot be too big and the lattice size should be as large as possible so as to get the results as accurate as possible. This conclusion is in agreement with the exponent variations in Table I, where the values of the exponent ν, for example, deviate dramatically from the exact one when $m=5$ (not listed) and the final estimations of the exponents are averaged over m not bigger than 4. However, this is not sufficient for obtaining considerably accurate exponent estimations. As discussed previously, decreasing the sweep rate leads the system to be closer to the fixed point and then more reliable estimates of the exponents. So with the lattice sizes as large as possible, accuracies of the exponents in Table I may then be further improved by decreasing the sweep rate and using more samples.

IV. SUMMARY

We have applied the extended MCRG to the two-dimensional three-state Potts model to study the continuous phase transition. The two lattices are respectively renormalized successively and the correlation functions are matched between the two systems having the same lattice sizes and the exponents ν, r, and then z have been calculated. Due to the linearly varying temperature that drives the system out of equilibrium, the method can effectively overcome the critical slowing down which pledges in equilibrium situations. Although this work is a direct application of our previous method, by using substantially more samples, the precisions of the exponents obtained have been improved by one digit. Moreover, the dynamic exponent $z=2.171(62)$ makes the results of the MCRG catalog overlap the other two catalogs, leading to a converging result. Combining our present result of $z=2.171(62)$ with the previously obtained $z=2.15(13)$ for $q=2$, one sees that the extension of weak universality hypothesis to dynamic critical behavior seems reliable and z appears to be q independent within statistical errors. The remaining small deviations among the existing results for identical and different q may arise from systematic and statistical errors since the present available methods are all to some extent approximate [64] and systematic RG results have not yet been available. This strongly calls for analytic dynamic RG results for such simple models to resolve such basic questions as the dynamic critical exponent and universality classes, even after nearly four decades of studies on critical dynamics.

As additional contributions to the method, we have determined the specific heat and shown that it follows its dynamic scaling form with respect to the temperature sweep rate correctly even in the present nonequilibrium conditions, as does the scaling form of the order parameter. The order parameter exponent β has also been determined from the satisfactory collapse of the rescaled order parameter vs the rescaled temperature. With ν and β in hand, all the other static critical exponents have been determined with considerable accuracy. Our results thus further confirm the method and its theory and indicate that we can apply this method to a system with unknown critical exponents, both dynamic and static. The critical temperature can also be determined within the method. We have also discussed both quantitative and qualitative the variations of V_E and V_M with the lattice size and the sweep rate. They all show self averaging in that they both decrease with increasing lattice sizes albeit in different manners, viz., the former follows possibly the equilibrium finite-size relation but not the latter. The sweep rate has a slight effect on V_E but significantly affects V_M. Consequently, to improve the accuracy of the exponents, the first step is to improve the accuracy of G_{nn}, so we need to improve the accuracies of both V_E and V_M by increasing the lattice size, and the RG iteration number cannot be too big. The second step is to decrease the sweep rate so as to drive the system to be closer to the fixed point and get averages over more samples.

ACKNOWLEDGMENTS

This work was supported by the NCET of MOE, PRC, and the NNSFC (Grants No. 10374118 and No. 10625420).

[1] For a recent review, see M. Barmatz, I. Hahn, J. A. Lipa, and R. V. Duncan, Rev. Mod. Phys. **79**, 1 (2007).
[2] R. Guida and J. Zinn-Justin, J. Phys. A **31**, 8103 (1998), see also Ref. [1] for more recent ones.
[3] A. Haupt and J. Straub, Phys. Rev. E **59**, 1795 (1999).
[4] F. Jasch and H. Kleinert, J. Math. Phys. **42**, 52 (2001).
[5] M. Campostrini, M. Hasenbusch, A. Pelissetto, P. Rossi, and E. Vicari, Phys. Rev. B **63**, 214503 (2001).
[6] J. A. Lipa, J. A. Nissen, D. A. Stricker, D. R. Swanson, and T. C. P. Chui, Phys. Rev. B **68**, 174518 (2003).
[7] P. C. Hohenberg and B. I. Halperin, Rev. Mod. Phys. **49**, 435 (1977).
[8] V. Dohm, Phys. Rev. B **73**, 092503 (2006), and references therein.

[9] For a review, see R. Folk and G. Moser, J. Phys. A **39**, R207 (2006).
[10] N. V. Antonov and A. N. Vasil'ev, Theor. Math. Phys. **60**, 671 (1984).
[11] V. V. Prudnikov, A. V. Ivanov, and A. A. Fedorenko, JETP Lett. **66**, 835 (1997)[Pis'ma Zh. Eksp. Teor. Fiz. **66**, 793 (1997).; A. S. Krinitsyn, V. V. Prudnikov, and P. V. Prudnikov, Theor. Math. Phys. **147**, 561 (2006).[Rev. Mex. Fis. **147**, 137 (2006)].
[12] S. Wansleben and D. P. Landau, Phys. Rev. B **43**, 6006 (1991); P. Grassberger, Physica A **214**, 547 (1995).
[13] F. Zhong, Phys. Rev. E **73**, 047102 (2006).
[14] Z. Racz and M. F. Collins, Phys. Rev. B **13**, 3074 (1976); G. F. Mazenko and O. T. Valls, *ibid.* **24**, 1419 (1981); Martin-D. Lacasse, J. Viñals, and M. Grant, *ibid.* **47**, 5646 (1993); Z. B. Li, L. Schulke, and B. Zheng, Phys. Rev. Lett. **74**, 3396 (1995); F. Wang, N. Hatane, and M. Suzuki, J. Phys. A **28**, 4543 (1995); B. Dammann and I. D. Reger, Z. Phys. B **98**, 97 (1995); M. P. Nightingale and H. W. J. Blöte, Phys. Rev. Lett. **76**, 4548 (1996).
[15] D. P. Landau and K. Binder, *A Guide to Monte Carlo Simulations in Statistical Physics* (Cambridge University Press, Cambridge, England, 2000).
[16] R. B. Potts, Proc. Cambridge Philos. Soc. **48**, 106 (1952); for a review, see F. Y. Wu, Rev. Mod. Phys. **54**, 235 (1982).
[17] G. R. Golner, Phys. Rev. B **8**, 3419 (1973); K. P. Zia and D. J. Wallace, J. Phys. A **8**, 1495 (1975); R. G. Priest and T. C. Lubensky, Phys. Rev. B **13**, 4159 (1976); **14**, 5125 (1976); D. J. Amit, J. Phys. A **9**, 1441 (1976).
[18] R. J. Baxter, J. Phys. C **6**, L445 (1973).
[19] P. G. de Gennes, Phys. Lett. **30A**, 454 (1969).
[20] M. Weger and J. B. Goldberg, *Solid State Physics* (Academic, New York, 1973), Vol. 28, p. 2.
[21] C. M. Fortuin and P. W. Kasteleyn, Physica (Amsterdam) **57**, 536 (1972); A. B. Harris, T. C. Lubensky, W. K. Holcomb, and C. Dasgupta, Phys. Rev. Lett. **35**, 327 (1975).
[22] M. E. Fisher, Phys. Rev. Lett. **40**, 1610 (1978).
[23] S. F. Edwards and P. W. Anderson, J. Phys. F **5**, 965 (1975).
[24] A. J. McKane, J. Phys. G **3**, 1165 (1977).
[25] A. N. Berker, S. Ostlund, and F. A. Putnam, Phys. Rev. B **17**, 3650 (1978).
[26] R. J. Baxter, *Exactly Solved Models in Statistical Mechanics* (Academic, London, 1982).
[27] L. da Silva, E. Mendonca Fleury Curado, S. Coutinho, and W. A. Martinez Morgado, Phys. Rev. B **53**, 6345 (1996); P. N. Timonin, J. Exp. Theor. Phys. **99**, 1044 (2004); R. J. Baxter, Phys. Rev. Lett. **94**, 130602 (2005); R. J. Baxter, J. Stat. Phys. **120**, 1 (2005); F. Y. Wu, Phys. Rev. Lett. **96**, 090602 (2006).
[28] O. F. de Alcantara Bonfim, J. E. Kirkham, and A. J. McKane, J. Phys. A **14**, 2391 (1981).
[29] G. Forgacs, S. T. Chui, and H. L. Frisch, Phys. Rev. B **22**, 415 (1980).
[30] K. Binder, J. Stat. Phys. **24**, 69 (1981).
[31] J. Tobochnik and C. Jayaprakash, Phys. Rev. B **25**, 4893 (1982).
[32] M. Aydin and M. C. Yalabik, J. Phys. A **17**, 2531 (1984).
[33] M. Aydin and M. C. Yalabik, J. Phys. A **18**, 1741 (1985).
[34] E. Domany, Phys. Rev. Lett. **52**, 871 (1984).
[35] L. D. Arcangelis and N. Jan, J. Phys. A **19**, L1179 (1986).
[36] S. Tang and D. P. Landau, Phys. Rev. B **36**, 567 (1987).
[37] O. F. de Alcantara Bonfim, Europhys. Lett. **4**, 373 (1987).
[38] C. Deroulers and A. P. Young, Phys. Rev. B **66**, 014438 (2002).
[39] L. Schülke and B. Zheng, Phys. Lett. A **204**, 295 (1995).
[40] K. Okano, L. Schülke, K. Yamagishi, and B. Zheng, Nucl. Phys. B **485**, 727 (1997).
[41] J.-B. Zhang, L. Wang, D.-W. Gu, H.-P. Ying, and D.-R. Ji, Phys. Lett. A **262**, 226 (1999).
[42] B. Zheng, Int. J. Mod. Phys. B **12**, 1419 (1998).
[43] H.-P. Ying, L. Wang, J.-B. Zhang, M. Jiang, and J. Hu, Physica A **294**, 111 (2001).
[44] R. D. da Silva, A. Nelson Alves, and J. R. Drugowich de Felicio, Phys. Lett. A **298**, 325 (2002).
[45] R. H. Swendsen and J. S. Wang, Phys. Rev. Lett. **58**, 86 (1987).
[46] R. P. Bikker and G. T. Barkema, Phys. Rev. E **62**, 5830 (2000).
[47] C. F. Baillie and P. D. Coddington, Phys. Rev. B **43**, 10617 (1991).
[48] N. Jan, L. L. Moseley, and D. Stauffer, J. Stat. Phys. **33**, 1 (1983).
[49] H. K. Janssen, B. Schaub, and B. Schmitmann, Z. Phys. B: Condens. Matter **73**, 539 (1989).
[50] M. Suzuki, Prog. Theor. Phys. **51**, 1992 (1974).
[51] F. Zhong and Z. F. Xu, Phys. Rev. B **71**, 132402 (2005).
[52] K. G. Wilson, Rev. Mod. Phys. **55**, 583 (1983).
[53] S. K. Ma, Phys. Rev. Lett. **37**, 461 (1976).
[54] R. H. Swendsen, Phys. Rev. Lett. **42**, 859 (1979).
[55] J. Tobochnik, S. Sarker, and R. Cordery, Phys. Rev. Lett. **46**, 1417 (1981).
[56] S. L. Katz, J. D. Gunton, and C. P. Liu, Phys. Rev. B **25**, 6008 (1982).
[57] F. Zhong, Phys. Rev. B **66**, 060401(R) (2002).
[58] Fan Zhong and Jinxiu Zhang, Phys. Rev. E **51**, 2898 (1995).
[59] N. Metropolis, M. N. Rosenbluth, A. Teller, and E. Teller, J. Chem. Phys. **21**, 1087 (1953).
[60] See, e.g., S. K. Ma, *Modern Theory of Critical Phenomena* (Benjamin, Reading, MA, 1976).
[61] M. S. S. Challa, D. P. Landau, and K. Binder, Phys. Rev. B **34**, 1841 (1986).
[62] M. E. Fisher and M. Randeria, Phys. Rev. Lett. **56**, 2332 (1986).
[63] A. Milchev, K. Binder, and D. W. Heermann, Z. Phys. B **63**, 521 (1986).
[64] K. Binder, Rep. Prog. Phys. **60**, 487 (1997).